

# Index Profile Design for High-Bandwidth W-Shaped Plastic Optical Fiber

Keita Takahashi, Takaaki Ishigure, *Member, IEEE*, and Yasuhiro Koike, *Member, IEEE*

**Abstract**—Modal dispersion in plastic optical fibers with W-shaped refractive index profiles (W-shaped POFs) is investigated. The authors focus on the effect of the refractive index valley at the boundary of core and cladding on the group delay. In this paper, particularly, the relationship between the depth of the index valley and the modal dispersion is highlighted. In order to analyze the relationship precisely, the authors prepare the W-shaped POFs with a high numerical aperture (NA  $\sim 0.25$ ), which are expected to show the effect of W-shaped profile more clearly than the W-shaped POFs with an NA of 0.2. As a result, the modal dispersion is strongly dependent on the depth of the index valley, which means that the control of the index valley is required, in order for minimum modal dispersion. Furthermore, by evaluating the output pulsewidth from the W-shaped POFs, the authors design the optimum index valley for the maximum bandwidth performance.

**Index Terms**—Modal dispersion, numerical aperture (NA), plastic optical fiber (POF), W-shaped index profile.

## I. INTRODUCTION

GROWING interests in fiber to the home (FTTH) and home networks are requiring more bandwidth not only for long-reach networks but also for short- and middle-reach networks. In long distance backbone networks, silica-based single-mode optical fiber is adopted widely because of its high bandwidth and low attenuation. However, because of the small core diameter of single-mode fibers (approximately 10  $\mu\text{m}$ ), alignment in optical couplings and fiber connections require high accuracy, which increases the total system cost of the single-mode fiber links. In recent years, silica-based multimode fibers (MMFs) have been utilized for Gigabit Ethernet and 10-Gb Ethernet [1]. The large diameter of silica-based MMFs (50- or 62.5-  $\mu\text{m}$  core) relaxes the accuracy in fiber alignment.

On the other hand, plastic optical fibers (POFs) with much larger core (120–1000  $\mu\text{m}$ ) than silica fibers are expected to be utilized as media for office and home networks (middle- or short-reach networks), because its large core and great mechanical flexibility allow for easy network installation. For high-speed optical links greater than several gigabit per second, photodiodes with a small detection area have to be used. In order to retain high coupling efficiency between the photodiode

and POFs, the large core of POFs is rather disadvantageous. Furthermore, we experimentally observed that the bending loss of POFs can be dramatically reduced when the core diameter is smaller than 200  $\mu\text{m}$  [2]. Thus, the optimization of the core diameter of POFs is examined. However, the great mechanical flexibility of POFs regardless of the core diameter is still advantageous for the fiber installation process. Therefore, POFs with great mechanical flexibility can dramatically decrease the total system cost.

We have proposed a high-bandwidth graded index (GI) POF that has a quadratic refractive index profile in the core region, and have demonstrated its high-bandwidth performance by forming an optimum refractive index profile [3], [4]. Since more than 50 000 modes propagate in POFs with large core ( $\sim 500 \mu\text{m}$ ), modal dispersion management is a key technology. In order to minimize the modal dispersion, we have proposed a W-shaped POF with a quadratic index profile in the radial direction followed by an index valley at the core-cladding boundary [5]. We have confirmed theoretically and experimentally that the group delay of higher order modes in the W-shaped POFs is decreased significantly by the refractive index valley. We have also confirmed that a W-shaped profile provides a modal dispersion improvement compared to those of the GI POFs (flat cladding) over a wide range of index exponent  $g$ , the quadratic parameter for the index profile of the GI and the W-shaped POFs [6]. The modal dispersion improvement by a W-shaped index profile has been already reported by Okoshi *et al.* [7]–[9] about 30 years ago, and very recently, similar results were also reported in [10]. They showed the effect of W-shaped index profiles on modal dispersion only theoretically, where only small numbers of modes ( $\sim 20$ ) were managed. However, we experimentally demonstrated for the first time in [5] that W-shaped index profiles are effective in reducing modal dispersion even in POFs that support huge number of modes ( $\sim 50\,000$ ).

However, in recent reports of the W-shaped POF [5], [6], the depth of the refractive index valley has been fixed to almost constant. There, the relationship between the depth of refractive index valley and the modal dispersion improvement was not investigated. The group delay of higher order modes in the W-shaped POFs is strongly influenced by the refractive index valley at the core-cladding boundary. Therefore, the depth of refractive index valley is a key parameter for determining the optimum W-shaped index profile. In this paper, in order to design the optimum W-shaped index profile, we investigate the relationship between the depth of refractive index valley and the modal dispersion improvement and then design the optimum index valley.

Manuscript received November 25, 2005; revised March 29, 2006.

The authors are with the Faculty of Science and Technology, Keio University, Yokohama 223-8522, Japan, and also with the Japan Science and Technology Agency (JST) Exploratory Research for Advanced Technology and Solution-Oriented Research for Science and Technology (ERATO-SORST) project, Kawasaki 212-0054, Japan (e-mail: y09972@educ.cc.keio.ac.jp; ishigure@appi.keio.ac.jp; koike@appi.keio.ac.jp).

Digital Object Identifier 10.1109/JLT.2006.876090

TABLE I  
CLADDING CHARACTERISTICS OF THE FABRICATED GI AND THE W-SHAPED POFs

Fiber	GI POF	W-shaped POF		
	2, 4, 5	6	1, 3, 7	8
Feed ratio (BzMA:MMA)	0:1.0	0.06:0.94	0.1:0.9	0.13:0.87
Refractive index of cladding	1.492	1.496	1.498	1.501

## II. EXPERIMENTAL

### A. Fiber Preparation

We obtain the W-shaped POFs by drawing preforms in which the W-shaped refractive index profile is formed. The preform and fiber diameters are 22 and 0.75 mm, respectively. A detailed fabrication method of the W-shaped POFs is described in [6]. We control the refractive index profile of the quadratic part of the W-shaped POFs by adjusting the polymerization condition of the core region and by adjusting the inner diameter of the polymer tube for the cladding. Furthermore, we control the numerical aperture (NA) by varying the concentration of the dopant (diphenyl sulfide), which has a refractive index ( $n_d = 1.629$ ) higher than that of polymethyl methacrylate (PMMA;  $n_d = 1.492$ ), for the core polymerization. In the previous articles [5], [6], the refractive index of the copolymer tube was fixed to 1.498. The copolymer tube was obtained by fixing the feed ratio of benzyl methacrylate (BzMA) and MMA to 0.1:0.9 by weight, respectively. In this paper, by varying the feed ratio of BzMA to MMA from 0.13:0.87 to 0.06:0.94 by weight, the depth of index valley can be controlled. The cladding characteristics of fabricated fibers are shown in Table I.

### B. Refractive Index Profile

Refractive index profiles of the GI and the W-shaped POFs are experimentally measured by the transverse interferometric technique described in [11]. We have already confirmed that this method has the highest accuracy in measuring not only quadratic refractive index profiles but also W-shaped refractive index profiles formed over such a wide range.

We have already reported that the index profiles of the GI POFs can be controlled over a wide range by the interfacial-gel polymerization process [4]. Fig. 1 shows a representative refractive index profile of the W-shaped POF [5]. In order to investigate the relationship between the refractive index profile and the bandwidth performances of the GI and the W-shaped POFs, the refractive index profiles are approximated by the power law equation shown by [7]–[9]

$$n(r) = n_1 \left[ 1 - 2\rho\Delta \left( \frac{r}{a} \right)^g \right]^{\frac{1}{2}}, \quad 0 \leq r \leq a$$

$$= n_2, \quad r \geq a \quad (1)$$

where  $n_1$  and  $n_2$  are the refractive indexes of the core center and cladding, respectively,  $a$  is the core radius, and  $\Delta$  is the

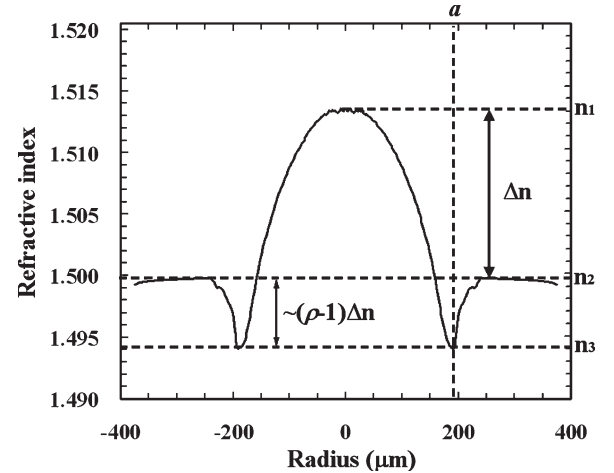


Fig. 1. Refractive index profile of the W-shaped POF.

relative index difference defined as

$$\Delta = \frac{n_1^2 - n_2^2}{2n_1^2}. \quad (2)$$

The parameter  $g$ , which is called index exponent, determines the refractive index profile of the quadratic part in the core region. We have already shown that the highest bandwidth is obtained in a PMMA-based GI POF at a wavelength of  $0.65 \mu\text{m}$  when the index exponent  $g$  is 2.45 in (1) [4]. The new parameter  $\rho$  in (1) signifies the depth of the index valley. When  $\rho$  is 1.0, the profile is the same as the conventional quadratic refractive index profile in the core followed by the flat index cladding, while the W-shaped index profile has the parameter  $\rho$  larger than 1.0. By (1),  $\rho$  is described as

$$\rho = \frac{n_1^2 - n_3^2}{n_1^2 - n_2^2} = \frac{\Delta_1}{\Delta} \quad (3)$$

where  $n_3$  is the refractive index just at the core-cladding boundary ( $r = a$ ), and  $\Delta$  is the relative index difference between core center and core-cladding boundary, which is defined as

$$\Delta_1 = \frac{n_1^2 - n_3^2}{2n_1^2}. \quad (4)$$

Thus,  $\rho$  indicates the ratio of the relative index difference. Therefore,  $n_1$ ,  $n_2$ , and  $n_3$  are important parameters to determine the depth of refractive index valley. Particularly, in this paper, we control the parameters of  $n_1$  and  $n_2$ , by which the index valley parameter  $\rho$  is controlled.

### C. Bandwidth Measurement of GI and W-Shaped POFs

The bandwidth of the GI and the W-shaped POFs is measured by a time domain measurement method. In this method, an optical pulse is launched into a fiber by an InGaAlP laser diode at  $0.65\ \mu\text{m}$ , and the output pulse waveform is measured by an optical sampling oscilloscope (Hamamatsu C-8188-03). Due to a specific modulation technique for obtaining a narrow optical pulse with a full-width at half-maximum (FWHM) of 50 ps, the spectral width of the signal is as broad as 3 nm. After measuring the waveforms of input and output pulses, the frequency spectra of these pulse waveforms are calculated by the Fourier transform. Then, the  $-3\text{-dB}$  bandwidth of the GI and the W-shaped POFs is calculated by the deconvolution of the obtained frequency spectra.

The bandwidth performance of MMFs is strongly dependent on the launch condition. In silica-based MMF links, a restricted launch condition is proposed and utilized in current MMF links to achieve high bit rate transmission [12]. Although it can also be applied to large-core POFs, a mode coupling is of a great concern. We have already confirmed that the mode coupling is weak enough in PMMA-based GI POFs with a distance of 100 m or less by increasing its NA [13]. On the other hand, it has been reported that a strong mode coupling still exists in a low loss perfluorinated (PF) GI POF [14], [15] with a distance longer than that of the PMMA-based POF. Furthermore, many fiber junctions and statistic bendings are expected in the GI POF networks [16], which is another origin of the mode coupling. Due to the mode coupling, the optical energy of the low-order modes would be coupled to higher order modes, even if only the low-order modes are launched selectively by the restricted launch condition. Since these high-order modes can degrade the bandwidth performance of the GI POFs, the group delay difference among all the modes (from lowest to highest order), should be minimized by the refractive index profile [4]. Since the W-shaped index profiles are expected to minimize the group delay difference among all the modes, in this paper, the bandwidth measurement is carried out under the overfilled launch condition, as described in [17], and the group delay of all the modes is evaluated.

### D. Propagating Modal Analysis

We mention in the above section that the mode coupling strongly influences the bandwidth performance of the GI and the W-shaped POFs. Therefore, in order to compare the bandwidth performance of the W-shaped POF to that of the GI POF, it is important to estimate the mode coupling strength in these POFs. The mode coupling strength in the GI and the W-shaped POFs is investigated by two methodologies: differential mode delay (DMD) and launch condition dependence in near-field pattern (NFP). [17], [18].

These two measurements adopt the similar launch technique described as follows.

An optical pulse signal from a laser diode (LD) at  $0.65\text{-}\mu\text{m}$  wavelength is coupled to the GI and the W-shaped POF via a 1-m single-mode fiber in order to excite specified small mode groups. By scanning the position where the single-mode fiber probe is butted to the POF, from the core center to the periphery,

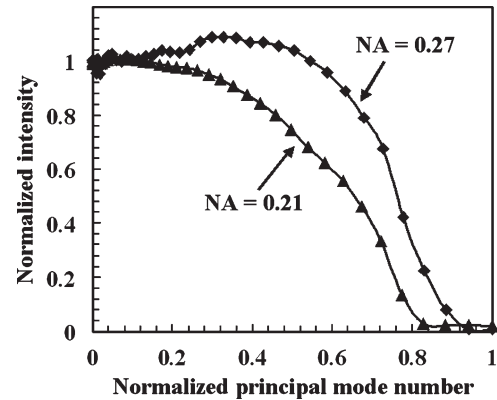


Fig. 2. Comparison of the mode power distributions (MPDs) from the two GI POFs with the same index exponent ( $g = 2.9$ ).

small groups of modes from low order to high order can be selectively launched.

After the POF transmission, by measuring the difference of time of flight among each mode group, we can observe the DMD. On the other hand, by measuring the NFP of each mode group, the launch condition dependence in NFP is obtained. The NFP of each mode group is measured by a charge-coupled device (CCD) camera set (Hamamatsu LEPAS-11) [17], [18].

### E. Differential Modal Attenuation (DMA) and Output Modal Power Distribution (MPD)

DMA is also an important characteristic that affects the bandwidth performance of POFs. Therefore, the DMA of the GI and the W-shaped POFs is directly measured using a method similar to the NFP measurement mentioned above. Small mode groups are launched selectively via a single-mode fiber probe in the same way as the DMD measurement. Here, because the local NA of the GI and the W-shaped POFs varies depending on the radial position, the coupling efficiency from the probe to the POFs also depends on the launched position. In order to compensate for the coupling efficiency of each mode group, a cutback method is adopted for the DMA measurement. Then, output MPDs are calculated from the DMA results.

## III. RESULTS AND DISCUSSION

### A. Refractive Index Profile of W-Shaped POF

In our previous article [6], we confirmed that the index valley of the W-shaped POFs contributed to the bandwidth improvement compared to conventional GI POFs over a wide range of  $g$ , when the NA and  $\rho$  were fixed to approximately 0.20 and 2.0, respectively; the depth of the index valley  $\rho$  is not varied in those samples. However, in order to determine the optimum “W-shaped” index profile, not only the  $g$  value but also the value of index valley  $\rho$  should be varied, and the relationship between the depth of index valley and bandwidth of the W-shaped POFs should be investigated.

In this paper, we focus on high-NA ( $\sim 0.25$ ) POFs in order to investigate the effect of the index valley in detail. Fig. 2 shows the normalized output MPD from the GI POFs with the same index exponent ( $g = 2.9$ ) and with the different NA. Fig. 2

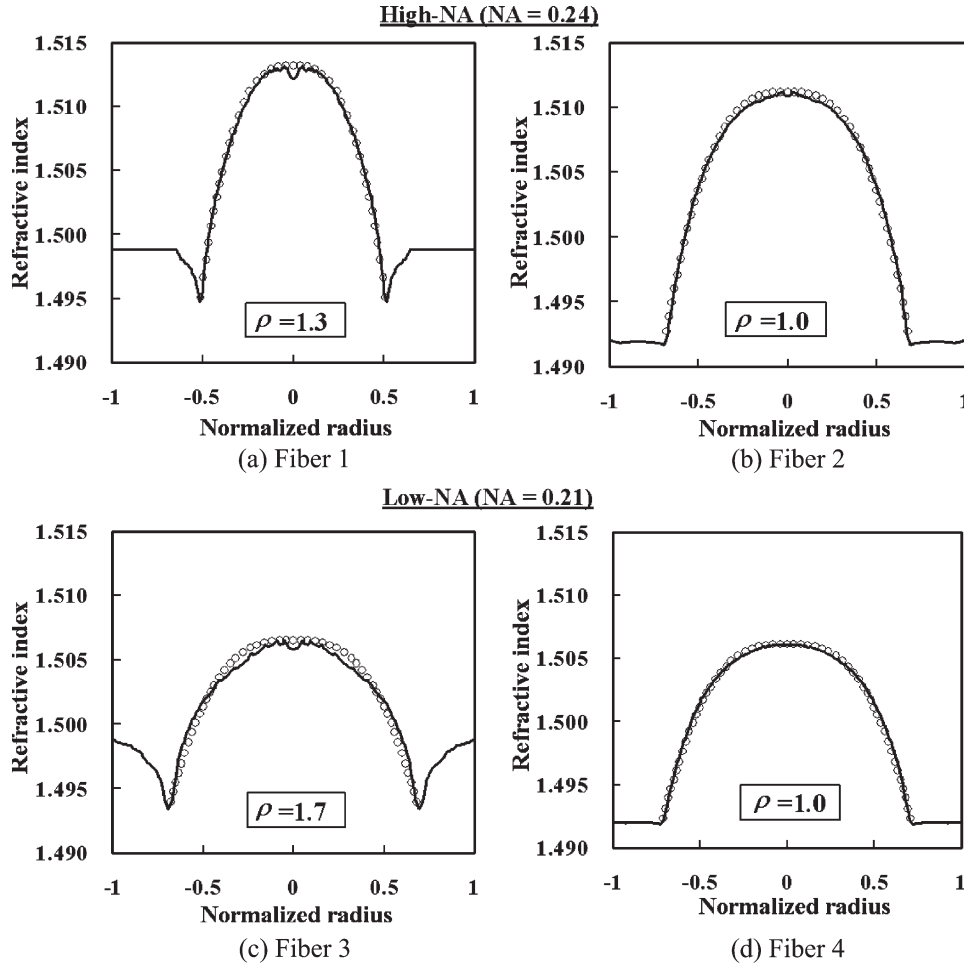


Fig. 3. Refractive index profiles of high-NA W-shaped (Fiber 1) and GI (Fiber 2) POFs, compared to those of low-NA W-shaped (Fiber 3) and GI (Fiber 4) POFs. The refractive index exponent of all POFs is the same value ( $g = 2.9$ ), as indicated by open circles (fitted to the power law form with  $g = 2.9$ ).

shows that the high-NA GI POF has a high output power in its high-order modes, compared to those of low-NA GI POF. This result means that a high optical power in the high-order modes is maintained even after a 100-m transmission, although both fibers have the same refractive index exponent  $g$ . Therefore, it can be seen that the output pulse broadening due to the modal dispersions of the GI and the W-shaped POFs are largely influenced by the NA.

The measured refractive index profile of the high-NA W-shaped POF (Fiber 1) is shown in Fig. 3(a). The NA of the newly fabricated W-shaped POF ( $NA = 0.24$ ) in Fig. 3(a) is higher than that ( $NA = 0.21$ ) of the conventional W-shaped POF [5], [6]. However, the depth of the index valley is smaller ( $\rho = 1.3$ ) by increasing the NA. Fig. 3(b) shows the refractive index profile of the high-NA GI POF (Fiber 2), which has almost the same NA and index exponent  $g$  ( $g = 2.9$ ) in the core region as those of Fiber 2. By comparing the bandwidth performance of these two fibers, the modal dispersion improvement in the high-NA W-shaped POF is experimentally confirmed.

**B. Bandwidth Performance of High-NA W-Shaped POF**

In order to investigate the effects of the depth of index valley on the bandwidth, the output waveform from Fiber 1 is compared to that from Fiber 2 (GI POF). Furthermore, the

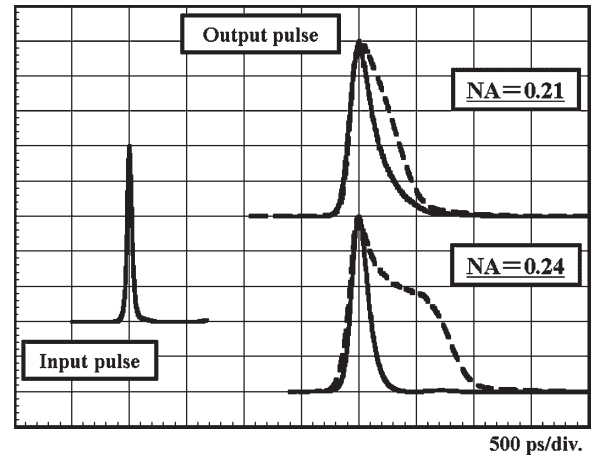


Fig. 4. Comparison of the measured output pulse waveforms from 100-m Fibers 1 to 4 at a wavelength of  $0.65 \mu\text{m}$ . Solid line: W-shaped POF Broken line: GI POF.

NA dependence of the bandwidth performance is compared between the GI and the W-shaped POFs by comparing the bandwidth of Fibers 1 and 2 ( $NA = 0.24$ ) as well as Fibers 3 and 4 ( $NA = 0.21$ ). Here, those fibers have almost the same index exponent  $g$  in their core regions. The results of 100-m POF samples are shown in Fig. 4. Estimated  $-3\text{-dB}$  bandwidth of

TABLE II  
COMPARISON OF  $-3$  dB BANDWIDTH BETWEEN THE GI AND THE W-SHAPED POFs SHOWN IN FIG. 4

Fiber NA	Sample Number	Index Profile	Bandwidth (GHz for 100m)
0.21	Fiber 4	GI	1.12
	Fiber 3	W-shape	1.68
0.24	Fiber 2	GI	0.65
	Fiber 1	W-shape	2.42

the fibers shown in Fig. 4 is summarized in Table II. In the case of the GI POFs, although the measured refractive index profiles of the two fibers are expressed by the same index exponent, a larger output pulse broadening is observed in the high-NA GI POF (Fiber 2). As we prove in the above section, high optical power in the high-order modes is maintained even after a 100-m transmission through the high-NA GI POF. Since the delay time of high-order modes is larger than that of low-order modes, because the  $g$  value ( $g = 2.9$ ) is larger than the optimum ( $g = 2.4$ ), the output pulse is much broader in the high-NA GI POF.

On the other hand, the output pulses from the W-shaped POFs are narrower than those of the GI POFs regardless of NA value. Particularly, in the case of the high-NA W-shaped POF (Fiber 1), the bandwidth (2.42 GHz for 100 m) is much higher than that (0.65 GHz for 100 m) of the GI POF (Fiber 2), despite the smaller index valley  $\rho$  ( $\rho = 1.3$ ) than that of the conventional W-shaped POF described in [5] ( $\rho = 1.7$ ). Thus, it is indicated that in the high-NA W-shaped POF, the index valley dramatically influences the modal dispersion and contributes significantly to the improvement in the bandwidth, as shown in Table II.

### C. Dependence of Modal Dispersion on Refractive Index Valley

In this section, the NA of the GI and the W-shaped POFs is fixed, and instead, the depth of the index valley is varied for investigating  $\rho$  value dependence of the bandwidth performance. The measured refractive index profiles of the W-shaped POFs (Fibers 6 to 8) with different index valley parameters ( $\rho = 1.2, 1.5,$  and  $1.8$ , respectively) are shown in Fig. 5. All fiber samples have the same NA (NA = 0.24), which is also the same as the NA of Fiber 5 (GI POF). In addition to the NA, the index exponent  $g$  of Fibers 5 through 8 is almost the same value (the  $g$  values of Fibers 5 to 8 are 4.4, 3.8, 4.1, and 4.1, respectively).

In order to quantitatively analyze the dependence of the modal dispersion on  $\rho$  in the W-shaped POFs, the mode coupling strength in the fibers has to be evaluated prior to the DMD analysis. As the strong mode coupling can allow the group delay of the modes to be averaged, the DMD results show no launch condition dependence in the fibers with such strong mode coupling.

The launch condition dependence of NFPs at the output end of the W-shaped and the GI POFs is measured to investigate the mode coupling strength. The results of these 100-m Fibers 5 to 8 are shown in Fig. 6. In all POFs, the observed spot sizes of the low-order modes are much smaller than the core

diameter, while explicit ring patterns are observed in the NFPs of the high-order modes. Thus, the remarkable differences in the NFPs between low- and high-order modes indicate that the mode coupling in these fibers is weak enough. Therefore, we can identify the group delay of each mode group in both high-NA GI and W-shaped POFs by the DMD measurement. Then, we investigate the relationship between the  $\rho$  value and the modal dispersion improvement.

The results of DMD measurements in both GI and W-shaped POFs are shown in Fig. 7. The W-shaped POFs shown in Fig. 5 have different index valley parameters  $\rho$ , while other parameters are almost the same. Therefore, the relationship between  $\rho$  and the modal dispersion improvement can be shown clearly by comparing the DMD results of those W-shaped POFs. The measured values of group delay in each mode group are shown by the peak position (shown by diamond) in each pulse. Here, the vertical position of each pulse is aligned to show that the peak of each pulse could indicate the group delay of the mode (group). The normalized principal mode number (in average) of the corresponding mode is shown in the vertical axis.

The DMD is calculated theoretically from the measured refractive index profiles by utilizing the Wentzel–Kramers–Brillouin (WKB) method that we adopted in [6]. In the calculation, only the quadratic part of the index profile in the core region is taken into account, as illustrated in [6]. The effects of cladding with flat refractive index and index valley are not taken into account. The calculated results are indicated in Fig. 7 by broken lines.

The index exponents  $g$  of those POFs are almost the same ( $g \approx 4.0$ ), which is deviated from the optimum value ( $g_{\text{opt}} = 2.4$ ) for the conventional GI POF [4]. This  $g$  value is more appropriate for analyzing the modal dispersion improvement due to the W-shaped profile than the  $g$  value close to 2.4, because the group delay of each mode group is clearly detected.

In the case of the GI POF (Fiber 5), a good agreement is observed between the calculated DMD curve and the measured values indicated by diamond. We have already confirmed this good agreement in the GI POFs [4], [17], even if the cladding effect is not taken into account for calculations. On the other hand, in the W-shaped POFs (Fibers 6 to 8), discrepancies between the measured and calculated DMD curves are observed, particularly in the higher order modes. Fig. 8 summarizes all the results shown in Fig. 7(b)–(d) in one figure to show the  $\rho$  dependence of DMD more clearly. Because the index exponents  $g$  of all the W-shaped POFs are almost the same, the calculated DMD curves of these fibers (all lines) are very close each other, as shown in Fig. 8. On the other hand, the discrepancies

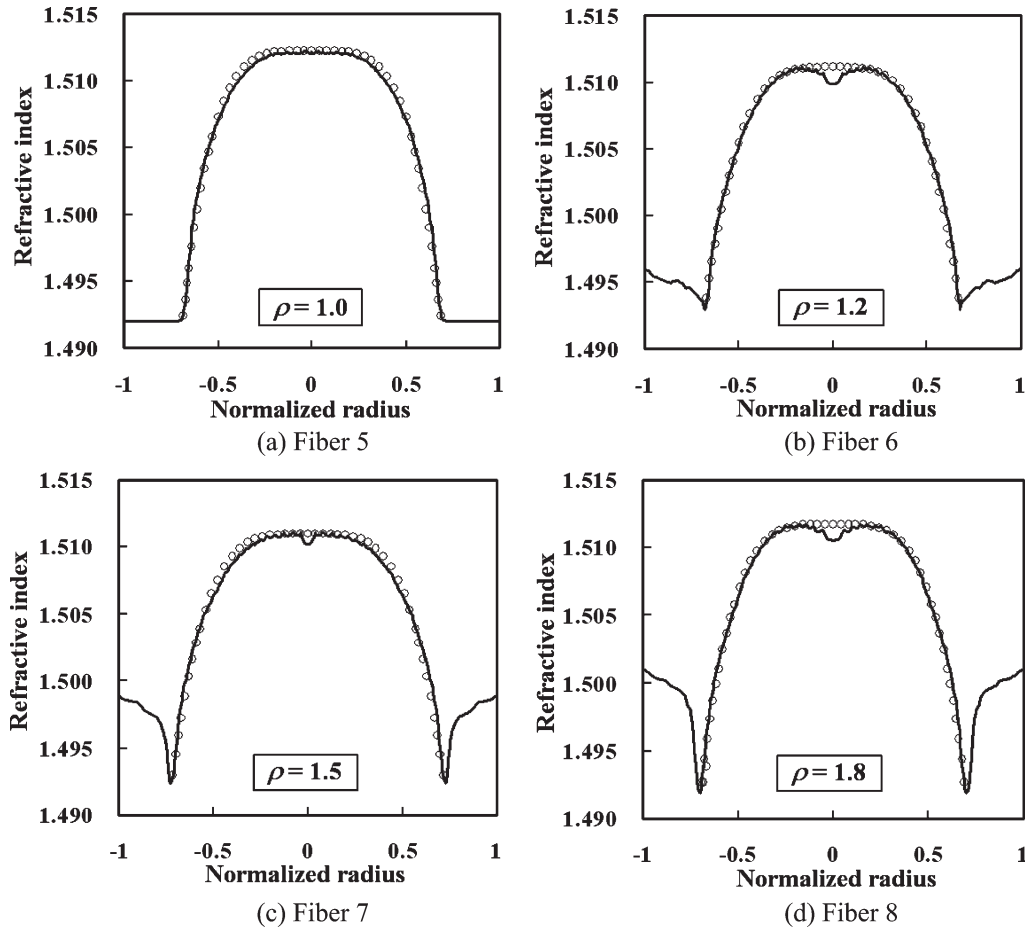


Fig. 5. Refractive index profiles of the GI and the W-shaped POFs with different depth of index valley. All fiber samples have almost the same NA ( $NA = 0.24$ ) and refractive index exponent (the  $g$  values of Fibers 5 through 8 are 4.4, 3.8, 4.1, and 4.1, respectively, as indicated by open circles, which show the best fitted profile to the power law form).

between measured and calculated DMD results are observed clearly in high-order modes, and with increasing the  $\rho$  value, larger discrepancies are observed. As mentioned in above, the calculated results are concerning neither flat index cladding nor index valley. Thus, the discrepancy between the measured and calculated results of the W-shaped POFs in Fig. 8 indicates the modal dispersion improvement due to the index valley. In general, the evanescent field of high-order modes is strongly influenced by the core-cladding boundary. Consequently, the group delay of the high-order modes are mainly decreased in the W-shaped POFs, as shown in Fig. 8. Thus, we demonstrate for the first time that the modal dispersion improvement due to W-shaped index profile has large  $\rho$  dependence.

#### D. Mode Power Distribution

We already proved in [6] that the higher order modes in the W-shaped POF were not attenuated but retained their optical power even after 100-m transmission. This tendency is observed more significantly in the W-shaped POFs than in the GI POFs. The relationship between the depth of the index valley and MPD should be investigated. In this paper, we calculate the normalized output intensity distribution in each mode group from the DMA results of Fibers 5 through 8, and then this relationship is evaluated.

The results of output intensity of each mode group from Fibers 5 and 8 are shown in Fig. 9. In the W-shaped POFs ( $\rho > 1.0$ ), the output intensity of higher order modes is higher than that in the GI POF. This tendency is consistent in the other two W-shaped POFs (Fibers 6 and 7). It is confirmed that the effect of strong output power in the higher order modes by a W-shaped index profile is independent on the depth of index valley.

#### E. Optimum Depth Index of Index Valley

It is found that a W-shaped index profile has two effects: One is group delay contraction, particularly in high-order modes, as shown in Fig. 7. With increasing the depth of index valley, group delay difference between the lowest and highest order modes is also decreased. Thus, the group delay contraction is a positive function for high bandwidth. The other effect is the strong optical confinement of high-order modes, which leads low attenuation in high-order modes. Since high-order modes generally have larger group delay than low-order modes in the GI and the W-shaped POFs, the strong optical confinement is a negative function for high bandwidth. Therefore, the optimum W-shaped index profile should be determined by considering both effects.

In this paper, we focus on the output pulse width for designing the optimum W-shaped index profile. The measured

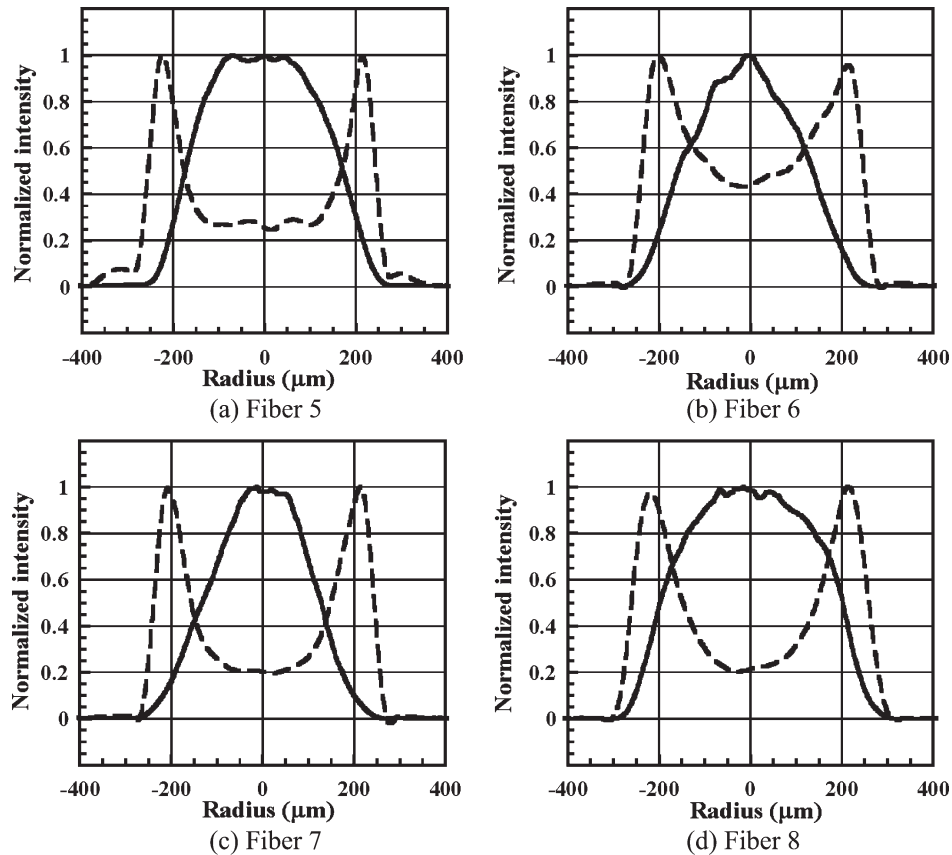


Fig. 6. Measured NIPs of low- and high-order modes from 100-m Fibers 5 to 8. Signal wavelength is  $0.65 \mu\text{m}$ . Solid Line:  $0\text{-}\mu\text{m}$  offset launch (low-order modes), Broken Line:  $240\text{-}\mu\text{m}$  offset launch (high-order modes).

output pulses from 100-m GI and W-shaped POFs (Fibers 5 to 8) are shown in Fig. 10 by solid lines. On the other hand, the output pulse waveforms are estimated by the convolution of input waveform and the impulse response function of the fiber obtained by the calculated group delay of each mode. A detailed calculation by the WKB method is described in [4], [6], and [19]. The calculated output pulse waveforms are also shown in Fig. 10. For obtaining the calculated waveforms, not only the group delay, but also the experimentally measured MPD (shown in Fig. 9), is taken into account. As shown in Fig. 10(a), relatively good agreement is observed in the GI POF (Fiber 5). We have already confirmed in [4] and [17] that the calculated output waveforms by the WKB method show good agreement with measured ones in many of the GI POFs if the MPDs are taken into consideration. On the other hand, calculated waveforms of the W-shaped POFs in Fig. 10 show disagreements with the measured waveforms, even if the MPD is taken into consideration (shown by closed circle). The disagreement is more clearly observed for larger  $\rho$  value. Since the index valley is not taken into consideration in the calculation, the disagreements shown in Fig. 10(b)–(d) correspond to the dispersion improvement due to the index valley.

Here, we focus on the effective pulsewidth  $2\sigma$ . The pulsewidth  $\sigma$  is the root-mean-square (rms) width, which is calculated by the following equation:

$$\sigma^2 = \frac{\int_{-\infty}^{+\infty} (t - \bar{t})^2 p(t) dt}{\int_{-\infty}^{+\infty} p(t) dt} \quad (5)$$

where  $p(t)$  is the output pulse waveform with respective time  $t$ , and  $\bar{t}$  is defined as

$$\bar{t} = \frac{\int_{-\infty}^{+\infty} tp(t) dt}{\int_{-\infty}^{+\infty} p(t) dt}. \quad (6)$$

The effective pulse broadening ( $\Delta 2\sigma$ ) through the POF transmission is calculated by (7)

$$\Delta(2\sigma) = \left( (2\sigma_{\text{out}})^2 - (2\sigma_{\text{in}})^2 \right)^{\frac{1}{2}} \quad (7)$$

where  $\sigma_{\text{out}}$  and  $\sigma_{\text{in}}$  are rms widths of output and input pulse waveforms, respectively.

In order to independently evaluate each of the two effects (the group delay contraction and the MPD), we calculate the effective pulse broadening  $\Delta 2\sigma$ , not only for the measured output pulses but also for calculated output pulses shown in Fig. 10.

Two different calculated waveforms are shown in Fig. 10(b)–(d). The waveforms shown by open circles are calculated by taking the MPD of the GI POF (shown in Fig. 9 by diamond) into account. On the other hand, the waveforms shown by closed circles are calculated by considering the measured MPD of each W-shaped POF. As mentioned in the previous section, the high-order modes in the GI POFs have less power than the same high-order modes in the W-shaped POFs. Thus, the pulses calculated with MPD of the GI POF (open circles) are narrower than the pulses calculated with MPD of the W-shaped

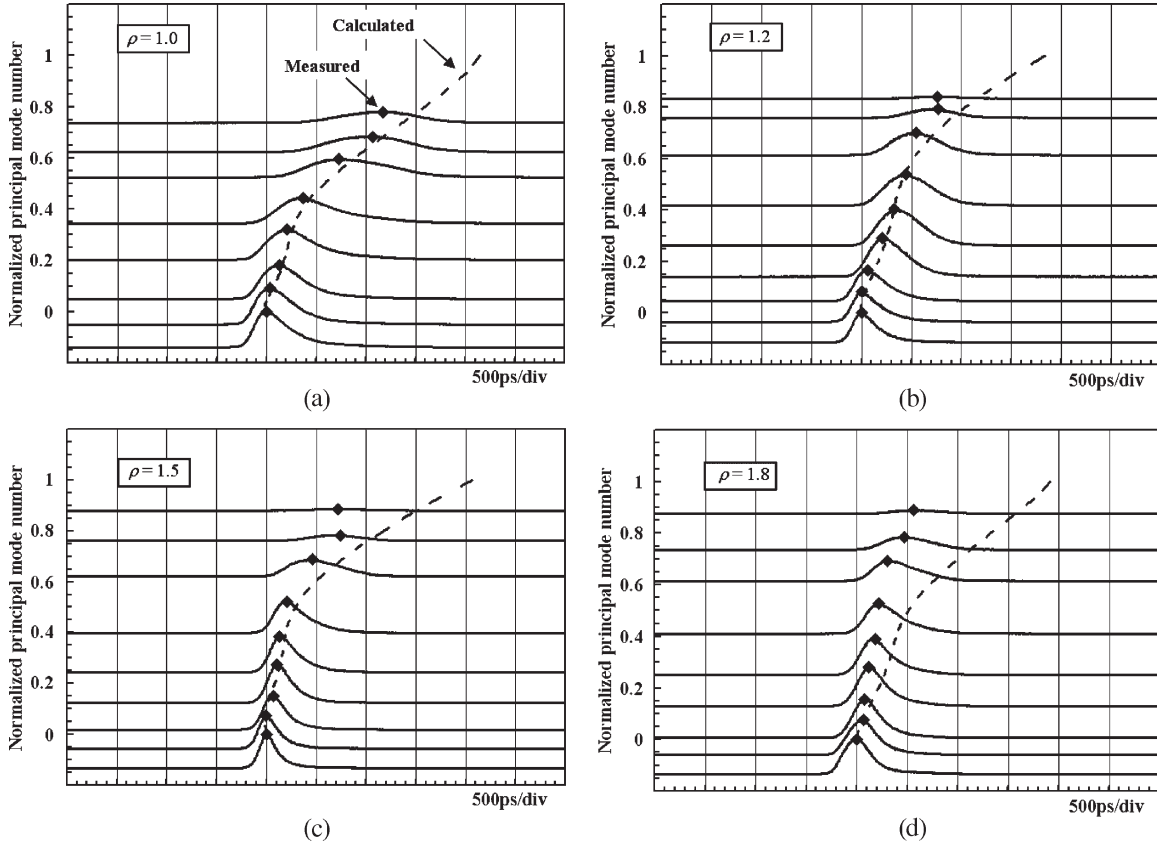


Fig. 7. Measured DMD after 100-m transmission through Fibers 5 to 8 at a wavelength of 0.65 μm. Broken lines: Calculated DMDs. Solid lines with plots: Measured DMDs.

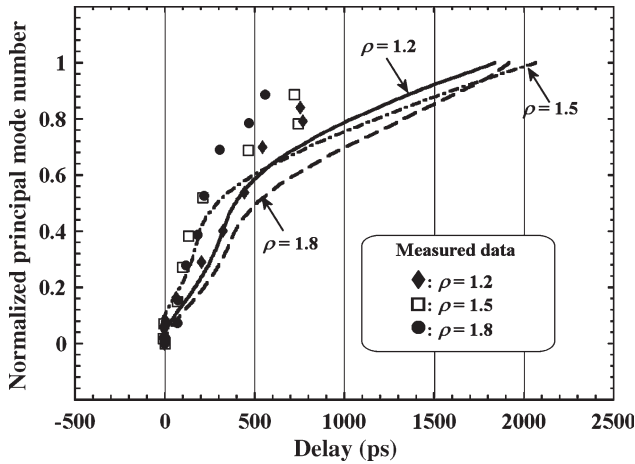


Fig. 8. Comparison of the measured DMDs after 100-m transmission through the W-shaped POFs (Fibers 6 to 8) with different index valley parameter shown in Fig. 7. Broken and solid lines: Calculated DMDs. Plots: Measured DMDs.

POF (closed circles) in Fig. 10(b)–(d). The effective pulse broadening calculated for these pulses are evaluated by plotting their ratios, which are defined by the following parameters:

$$P_1 = \frac{\Delta 2\sigma(W_{cal})}{\Delta 2\sigma(GI_{cal})} \quad (8)$$

$$P_2 = \frac{\Delta 2\sigma(measured)}{\Delta 2\sigma(W_{cal})} \quad (9)$$

$$P_3 = \frac{\Delta 2\sigma(measured)}{\Delta 2\sigma(GI_{cal})} \quad (10)$$

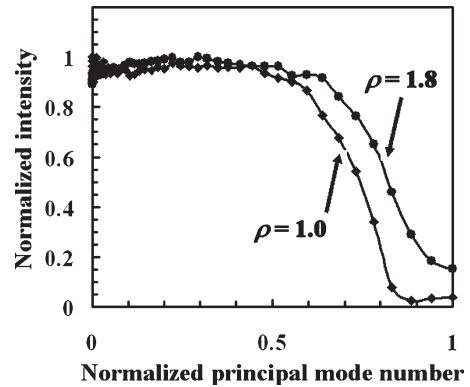


Fig. 9. Comparison of the output power distribution between the GI (Fiber 5, ρ = 1.0) and the W-shaped (Fiber 8, ρ = 1.8) POFs.

where  $\Delta 2\sigma(W_{cal})$ ,  $\Delta 2\sigma(GI_{cal})$ , and  $\Delta 2\sigma(measured)$  are the effective pulse broadenings calculated with the MPD of GI profile, and measured experimentally, respectively.

The parameters  $P_1$ ,  $P_2$ , and  $P_3$  with respect to the parameter  $\rho$  are shown in Fig. 11. As in Fig. 11, the parameter  $P_1$  shows the maximum value when  $\rho$  equals 1.2 and larger than 1, regardless of  $\rho$  value. From the aspect of MPD, W-shaped index profile is less effective for obtaining bandwidth higher than the GI POF.

The relationship between  $P_2$  and  $\rho$  highlights the contribution of the index valley to the group delay contraction



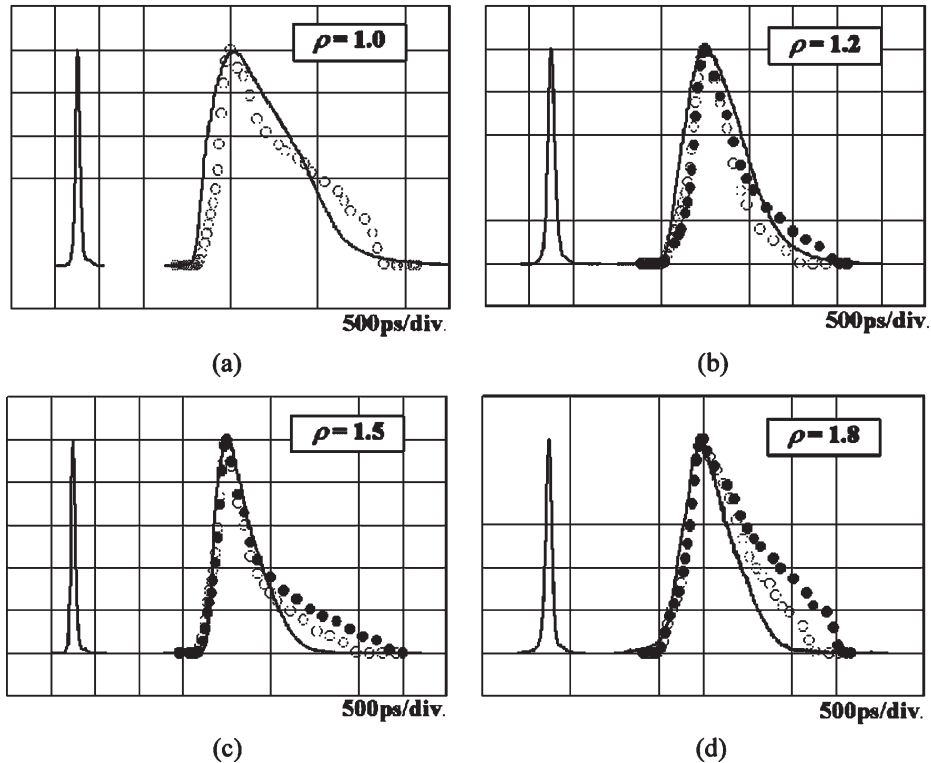


Fig. 10. Measured and calculated output pulse waveforms from 100-m Fibers 5 to 8 at a wavelength of  $0.65 \mu\text{m}$ . Solid line: measured waveform. Open circle: calculated waveform considering GI DMA. Closed circle: calculated waveform considering W-shaped DMA.

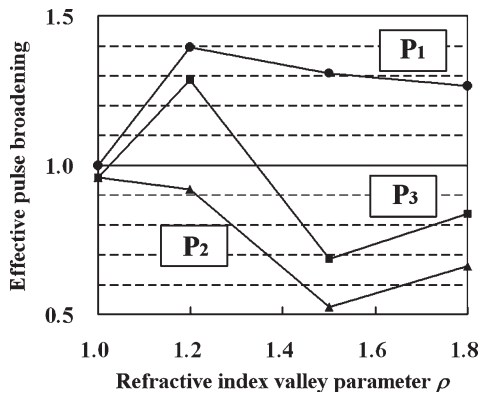


Fig. 11. Relationship between the ratio of effective pulse broadenings ( $P_1$ ,  $P_2$ , and  $P_3$ ) and the parameter  $\rho$ .

more clearly. The measured output pulse is narrower than the calculated pulse ( $P_2 < 1$ ) for all  $\rho$  values. This means that the W-shaped index profile is capable of decreasing the modal dispersion even compared to the normal GI profile. It should be noted that the group delay is minimum when  $\rho$  is 1.5, and significant group delay contraction is no longer obtained for  $\rho$  value larger than 1.5. Therefore, we can conclude that a  $\rho$  value of 1.5 is large enough for obtaining the bandwidth higher than the conventional GI POF ( $\rho = 1.0$ ).

For determining the optimum W-shaped index profile, the bandwidth improvement from the conventional GI POF should be evaluated. The effect of the output MPD is again discussed. In Fig. 11, the parameter  $P_3$  is plotted with respect to  $\rho$  values. When the parameter  $P_3$  equals 1, the group delay contraction

effect (positive for high bandwidth) is compensated by the MPD effect (negative for high bandwidth). The parameter  $P_3$  is smaller than 1 for the  $\rho$  value larger than 1.5. This indicates that the group delay contraction effect overcomes the MPD effect, if the  $\rho$  value is larger than 1.5. On the other hand, when  $\rho = 1.2$ ,  $P_3$  is larger than 1. In this case, as the index valley is so shallow that the group delay contraction effect is not stronger than the MPD effect.

From the results shown in Fig. 11, it is concluded that the  $\rho$  value should be as large as 1.5, but the value should not be larger than 1.5. Since the MPD effect is also depending on the NA of fibers [18], this optimum depth of the index valley is valid for the W-shaped POFs with an NA of approximately 0.25. The optimum W-shaped index profile for other NAs will be reported in the other paper.

#### IV. CONCLUSION

The relationship between the depth of the index valley and the modal dispersion improvement from the conventional GI POF is investigated using high-NA W-shaped POFs for the first time. In the high-NA W-shaped POFs, the index valley dramatically influences the modal dispersion and contributes significantly to the bandwidth improvement. The modal dispersion improvement in the W-shaped POFs is strongly dependent on the depth of index valley. On the other hand, in the W-shaped POFs ( $\rho > 1.0$ ), strong output intensity of higher order modes, which can degrade the bandwidth performance, is observed. It is also found that the output intensity of high-order modes is independent of the depth of index valley.

Considering the two key effects of W-shaped index profile on bandwidth performance, the optimum depth of the index valley is designed. We conclude that in the case where  $NA = 0.24$ , a  $\rho$  value of 1.5 is large enough to realize the bandwidth improvement due to the W-shaped index profile.

#### REFERENCES

- [1] P. Pepeljugoski, D. Kuchta, Y. Kwark, P. Pleunis, and G. Kuyt, "15.6-Gb/s transmission over 1 km of next generation multimode fiber," *IEEE Photon. Technol. Lett.*, vol. 14, no. 5, pp. 717–719, May 2002.
- [2] K. Makino, T. Ishigure, and Y. Koike, "Waveguide parameter design of graded-index plastic optical fibers for bending-loss reduction," *J. Lightw. Technol.*, vol. 24, no. 5, pp. 2108–2114, May 2006.
- [3] T. Ishigure, E. Nihei, and Y. Koike, "Graded-index polymer optical fiber for high speed data communication," *Appl. Opt.*, vol. 33, no. 19, pp. 4261–4266, Jul. 1994.
- [4] T. Ishigure, S. Tanaka, E. Kobayashi, and Y. Koike, "Accurate refractive index profiling in a graded-index plastic optical fiber exceeding gigabit transmission rates," *J. Lightw. Technol.*, vol. 20, no. 8, pp. 1449–1556, Aug. 2002.
- [5] T. Ishigure, H. Endo, K. Ohdoko, and Y. Koike, "High-bandwidth plastic optical fiber with W-refractive index profile," *IEEE Photon. Technol. Lett.*, vol. 16, no. 9, pp. 2081–2083, Sep. 2004.
- [6] T. Ishigure, H. Endo, K. Ohdoko, K. Takahashi, and Y. Koike, "Modal bandwidth enhancement in a plastic optical fiber by W-refractive index profile," *J. Lightw. Technol.*, vol. 23, no. 4, pp. 1754–1762, Apr. 2005.
- [7] K. Okamoto and T. Okoshi, "Computer-aided synthesis of the optimum refractive-index profile for a multimode fiber," *IEEE Trans. Microw. Theory Tech.*, vol. MTT-25, no. 3, pp. 213–221, Mar. 1977.
- [8] K. Oyama and T. Okoshi, "High-accuracy numerical data of propagation characteristics of a-power graded-core fibers," *IEEE Trans. Microw. Theory Tech.*, vol. 28, no. MTT-10, pp. 1113–1118, Oct. 1980.
- [9] K. Okamoto and T. Okoshi, "Analysis of wave propagation in optical fibers having core with a-power refractive-index distribution and uniform cladding," *IEEE Trans. Microw. Theory Tech.*, vol. MTT-24, no. 7, pp. 416–421, Jul. 1976.
- [10] D. Đonlagić, "Opportunities to enhance multimode fiber links by application of overfilled launch," *J. Lightw. Technol.*, vol. 23, no. 11, pp. 3526–3540, Nov. 2005.
- [11] Y. Ohtsuka and Y. Koike, "Determination of the refractive-index profile of light-focusing rods: Accuracy of a method using Interphako interference microscopy," *Appl. Opt.*, vol. 19, no. 16, pp. 2866–2872, Aug. 1980.
- [12] J. B. Schlager, M. J. Hackert, P. Pepeljugoski, and F. Gwinn, "Measurements for enhanced bandwidth performance over 62.5- $\mu\text{m}$  multimode fiber in short-wavelength local area networks," *J. Lightw. Technol.*, vol. 21, no. 5, pp. 1242–1255, May 2003.
- [13] K. Ohdoko, T. Ishigure, and Y. Koike, "Propagating mode analysis and design of waveguide parameters of GI POF for very short-reach network use," *IEEE Photon. Technol. Lett.*, vol. 17, no. 1, pp. 79–81, Jan. 2005.
- [14] S. E. Golowich, W. White, W. A. Reed, and E. Knudsen, "Quantitative estimates of mode coupling and differential modal attenuation in perfluorinated graded-index plastic optical fiber," *J. Lightw. Technol.*, vol. 21, no. 1, pp. 111–121, Jan. 2003.
- [15] T. Ishigure, Y. Koike, and J. W. Fleming, "Optimum index profile of the perfluorinated polymer based GI polymer optical fiber and its dispersion properties," *J. Lightw. Technol.*, vol. 18, no. 2, pp. 178–184, Feb. 2000.
- [16] J. Arrue, J. Zubia, G. Durana, and J. Mateo, "Parameters affecting bending losses in graded-index polymer optical fibers," *IEEE J. Sel. Topics Quantum Electron.*, vol. 7, no. 5, pp. 836–844, Sep./Oct. 2001.
- [17] T. Ishigure, M. Kano, and Y. Koike, "Which is a more serious factor to the bandwidth of GI POF: Differential mode attenuation or mode coupling?" *J. Lightw. Technol.*, vol. 18, no. 7, pp. 959–965, Jul. 2000.
- [18] T. Ishigure, K. Ohdoko, and Y. Koike, "Mode coupling control and new index profile of GI POF for restricted-launch condition in very-short reach networks," *J. Lightw. Technol.*, vol. 23, no. 12, pp. 4155–4168, Dec. 2005.
- [19] D. Marcuse, "Calculation of bandwidth from index profiles of optical fibers. 1: Theory," *Appl. Opt.*, vol. 18, no. 12, pp. 2073–2080, Jun. 1979.



**Keita Takahashi** was born in Tokyo, Japan, on August 11, 1981. He received the B.S. degree in applied physics and physico-informatics in 2004 and the M.S. degree in integrated design engineering, both from Keio University, Yokohama, Japan, in 2004.

He is currently with Nippon Telegraph and Telephone (NTT) Corporation, Chiba, Japan.



**Takaaki Ishigure** (M'00) was born in Gifu, Japan, on July 30, 1968. He received the B.S. degree in applied chemistry and the M.S. and Ph.D. degrees in material science, all from Keio University, Yokohama, Japan, in 1991, 1993, and 1996, respectively.

He is currently an Assistant Professor with Keio University. He has been concurrently a Group Leader of the Japan Science and Technology Agency (JST), Exploratory Research for Advanced Technology and Solution-Oriented Research for Science and Technology (ERATO-SORST) project. In 2005, he stayed

at the Department of Electrical Engineering, Columbia University, New York, NY, as a Visiting Research Scientist. His current research interests are in designing the optimum waveguide structure of high-bandwidth plastic optical fibers (POFs) and its system design.



**Yasuhiro Koike** (M'02–A'02–M'03) was born in Nagano, Japan, on April 7, 1954. He received the B.S., M.S., and Ph.D. degrees, all from Keio University, Yokohama, Japan, in 1977, 1979, and 1982, respectively, all in applied chemistry.

He has been a Professor with Keio University, where he developed the high-bandwidth GI polymer optical fiber. He has been concurrently the Director of the Japan Science and Technology Agency (JST) Exploratory Research for Advanced Technology and Solution-Oriented Research for Science and Technology (ERATO-SORST) project since 2005. He stayed as a Visiting Researcher at AT&T Bell Laboratories from 1989 through 1990.

Dr. Koike received the International Engineering and Technology Award of the Society of Plastics Engineers in 1994 and the Fujiwara Award in 2001.